Kwangil Kim; Unhyok Hong; Kwanhung Ri; Juhyon Yu

Construction of convergent adaptive weighted essentially non-oscillatory schemes for Hamilton-Jacobi equations on triangular meshes

Applications of Mathematics, Vol. 66 (2021), No. 4, 599–617

Persistent URL: http://dml.cz/dmlcz/148974

CONSTRUCTION OF CONVERGENT ADAPTIVE WEIGHTED ESSENTIALLY NON-OSCILLATORY SCHEMES FOR HAMILTON-JACOBI EQUATIONS ON TRIANGULAR MESHES

Kwangil Kim, Unhyok Hong, Kwanhung Ri, Juhyon Yu, Pyongyang

Received December 19, 2019. Published online May 11, 2021.

Abstract. We propose a method of constructing convergent high order schemes for Hamilton-Jacobi equations on triangular meshes, which is based on combining a high order scheme with a first order monotone scheme. According to this methodology, we construct adaptive schemes of weighted essentially non-oscillatory type on triangular meshes for non-convex Hamilton-Jacobi equations in which the first order monotone approximations are occasionally applied near singular points of the solution (discontinuities of the derivative) instead of weighted essentially non-oscillatory approximations. Through detailed numerical experiments, the convergence and effectiveness of the proposed adaptive schemes are demonstrated.

Keywords: Hamilton-Jacobi equation; first order monotone scheme; high order scheme; weighted essentially non-oscillatory scheme; adaptive scheme; convergence

MSC 2020: 35F21, 65M12, 65M50

1. Introduction

We study a numerical method for solving Hamilton-Jacobi (HJ) equations

$$u_t + H(\nabla u) = 0, \quad (x,t) \in \mathbb{R}^d \times (0,T], \tag{1.1}$$

$$u(x,0) = u_0(x), \quad x \in \mathbb{R}^d. \tag{1.2}$$

As one knows, it is especially important to resolve singularities such as the development of discontinuities in the solution derivative in composing numerical approximations for the Hamilton-Jacobi equation (1.1), (1.2). The first order monotone scheme by Crandal and Lions [4] is an important class of numerical methods for HJ equations and these schemes converge to viscosity solutions. But they are at most

DOI: 10.21136/AM.2021.0368-19

first order accurate and therefore acute parts of solutions are poorly resolved by these schemes.

In the last two decades, more accurate high order numerical methods for Hamilton-Jacobi equations have been extensively studied. In [12], the essentially non-oscillatory (ENO) scheme was proposed for the HJ equation, which is high order accurate and non-oscillatory near singularities of the solution. Weighted essentially non-oscillatory (WENO) schemes are representative high order schemes applied to convection dominated problems as well as HJ equations [15], [8], [16], [10], [5], [13], [17], [7], [18]. Applying a weighted convex combination in the reconstruction process to the derivative, WENO schemes achieve high order accuracy in the smooth region of the solution and give non-oscillatory and sharp approximations near singularities.

On the other hand, despite satisfactory numerical properties, few theoretical results on convergence are known for high order numerical methods [15]. In general, the convergence of high order schemes could not be expected for some HJ equations, including the problems with nonconvex Hamiltonians and Lipschitz continuous initial conditions [9]. The high order WENO scheme is based on combining the consistent monotone numerical Hamiltonian with the high order WENO approximation of derivative. So, it is difficult to ensure the convergence of WENO schemes only by the reconstruction of derivative based on pure interpolation, without considering properties of various types of HJ equations [9].

By adequately modifying a high order scheme, one could construct a new scheme which inherits good numerical properties of the high order scheme and, at the same time, strictly converges to the solution of the Hamilton-Jacobi equation. In [9], the authors constructed adaptive finite difference schemes of WENO type for the Hamilton-Jacobi equation by combining a high order WENO scheme with a first order monotone one, which achieves high order accuracy and converges to the exact solution. In [11], [2], the authors proposed filtered schemes based on a combination of high order and first order monotone schemes through filtered function and proved its convergence. Similar studies were performed in [14], [3] for hyperbolic conservation laws.

In this paper, we study problems of constructing convergent high order schemes on triangular meshes for the Hamilton-Jacobi equation. In Section 2, we propose a method of constructing the schemes of high order type on triangular meshes for the Hamilton-Jacobi equation by combining a high order approximation with a first order monotone one and discuss the convergence of the scheme. Section 3 is concerned with constructing adaptive schemes of WENO type on triangular meshes. Especially adaptive algorithms blending the high order WENO approximation with the first order one are proposed for nonconvex HJ equations. A singularity indicator is introduced on a triangular mesh, which acts as an indicator of identifying singularities in the solution. Detailed numerical experiments are performed to demonstrate the effectiveness of the adaptive schemes in Section 4.

2. Construction of adaptive high order schemes on triangular meshes

In this section, we construct adaptive high order schemes on triangular meshes based on combining a high order approximation with a first order monotone one and discuss the convergence of the scheme.

2.1. Construction of the scheme. Assume that the following holds for the HJ equation (1.1), (1.2):

(A_1) u_0 is a bounded Lipschitz continuous function and therefore there exists a constant L_0 satisfying the condition

$$|u_0(x) - u_0(y)| \leqslant L_0|x-y| \quad \forall\, x, y \in \mathbb{R}^d. \tag{2.1}$$

(A_2) The Hamiltonian H is a bounded Lipschitz continuous function in $\mathbb{R}^d$ and therefore there exists a constant L_H satisfying the condition

$$|H(p) - H(q)| \leqslant L_H|p-q| \quad \forall\, p, q \in \mathbb{R}^d. \tag{2.2}$$

On the above assumptions, there exists a unique viscosity solution of the equation (1.1), (1.2) which is bounded and Lipschitz continuous [4]. Here we consider the two-dimensional case ($d=2$). For regular triangulations T_h of $\mathbb{R}^2$, h_T is the diameter of the triangle T in T_h and $h = \sup\limits_{T\in T_h} h_T$. We define a spatial mesh G_h consisting of all division nodes named by their indices. Nodes are identified by their indices. We denote the triangles that have a common vertex $i \in G_h$ by $T_{i,j}$, $j = 1, \ldots, N_i$. They are enumerated counterclockwise. The semidiscrete first order monotone and high order schemes are written as

$$\frac{\mathrm{d}u_i(t)}{\mathrm{d}t} + \widehat{H}(\nabla^M u_{T_{i,1}}, \nabla^M u_{T_{i,2}}, \ldots, \nabla^M u_{T_{i,N_i}}) = 0, \quad i \in G_h, \tag{2.3}$$

$$\frac{\mathrm{d}u_i(t)}{\mathrm{d}t} + \widehat{H}(\nabla^H u_{T_{i,1}}, \nabla^H u_{T_{i,2}}, \ldots, \nabla^H u_{T_{i,N_i}}) = 0, \quad i \in G_h. \tag{2.4}$$

Here $\widehat{H}(\cdot)$ is a numerical Hamiltonian satisfying the conditions of consistency and monotonicity, and $\nabla^M u_{T_{i,j}}$ and $\nabla^H u_{T_{i,j}}$ denote the first and high order approximations of the derivative of u on the triangle $T_{i,j}$, $j = 1, \ldots, N_i$, respectively.

We define a semidiscrete scheme based on adaptive combinations of high and first order approximations of the derivative as

$$\frac{\mathrm{d}u_i(t)}{\mathrm{d}t} + \widehat{H}(\{\lambda_i(t)\nabla^H u_{T_{i,j}}(t) + (1-\lambda_i(t))\nabla^M u_{T_{i,j}}(t)\}_{j=\overline{1,N_i}}) = 0, \quad i \in G_h. \tag{2.5}$$

Here $\lambda_i(t) \in [0,1]$ is a blending coefficient depending on the node and the time level.

The reasonable selection of the blending coefficient $\lambda_i(t)$ makes it possible to construct a convergent scheme achieving the high order accuracy. In general, from the high order accuracy requirement, the blending coefficient should be taken as 1 in the smooth region of the solution (high order scheme) and in the singular parts of the solution, the blending coefficient takes the value in $[0,1]$ according to the convergence condition. As the solution depends on the time, the position of singular points also varies on the time and therefore the blending coefficient in (2.5) depends on the time. The question of selecting the blending coefficient is furthermore concretely discussed in Section 3.

For the time discretization, we use the strong stability preserving the (SSP) third order Runge-Kutta method [6] with a time step $\Delta t = T/N_T$. The full-discrete scheme is as follows:

For $i \in G_h$, $n = 0, 1, \ldots, N-1$,

$$\begin{cases} u_i^{n,1} = u_i^n - \Delta t \widehat{H}(\{\nabla u_{T_{i,j}}^n\}_{j=\overline{1,N_i}}), \quad u_i^0 = u_0(x_i), \\ u_i^{n,2} = \dfrac{3}{4}u_i^n + \dfrac{1}{4}u_i^{n,1} - \dfrac{1}{4}\Delta t \breve{H}(\{\nabla u_{T_{i,j}}^{n,1}\}_{j=\overline{1,N_i}}), \\ u_i^{n+1} = \dfrac{1}{3}u_i^n + \dfrac{2}{3}u_i^{n,2} - \dfrac{2}{3}\Delta t \breve{H}(\{\nabla u_{T_{i,j}}^{n,2}\}_{j=\overline{1,N_i}}). \end{cases} \tag{2.6}$$

Here $\nabla u_{T_{i,j}}^{n,l} = \lambda_i^{n,l}\nabla^H u_{T_{i,j}}^{u,l} + (1-\lambda_i^{n,l}\nabla M u_{T_{i,j}}^{n,l})$, $j = 1, \ldots, N_i$, $l = 0, 1, 2$ ($u^{n,0} = u^n$) and $\lambda_i^{n,l} \in [0,1]$ is the blending coefficient taken according to the node and the time level.

2.2. Convergence of the scheme (2.6)**.** In order to verify the convergence of the scheme (2.6), we first consider the following first order monotone scheme using the SSP third order Runge-Kutta time discretization: For $i \in G_h$, $n = 0, 1, \ldots, N-1$,

$$\begin{cases} v_i^{n,1} = v_i^n - \Delta t \widehat{H}(\{\nabla^M v_{T_{i,j}}^n\}_{j=\overline{1,N_i}}), \quad v_i^0 = u_0(x_i), \\ v_i^{n,2} = \dfrac{3}{4}v_i^n + \dfrac{1}{4}v_i^{n,1} - \dfrac{1}{4}\Delta t \breve{H}(\{\nabla^M v_{T_{i,j}}^{n,1}\}_{j=\overline{1,N_i}}), \\ v_i^{n+1} = \dfrac{1}{3}v_i^n + \dfrac{2}{3}v_i^{n,2} - \dfrac{2}{3}\Delta t \breve{H}(\{\nabla^M v_{T_{i,j}}^{n,2}\}_{j=\overline{1,N_i}}). \end{cases} \tag{2.7}$$

We denote unit vectors from the point $i \in G_h$ towards its neighboring points by $n_{i,j}$, $j = 1, 2, \ldots, N_i$, which are enumerated in the counterclockwise direction. The length of the line segment connecting the points i and j is denoted by $\delta_{i,j}$ and the angle between the two vectors $n_{i,j}$ and $n_{i,j+1}(n_{n,N_i+1} = n_{i,1})$ by $\theta_{i,j}$. We also denote the set of all neighboring points of the point $i \in G_h$ by $v_i \subset G_h$ and the $n_{i,j}$-directional derivative of the piecewise first order function v defined on the partition T_h by $\partial_{i,j}v$, $j = 1, \ldots, N_i$. Then we have

$$\partial_{i,j}v = (v_{i_j} - v_i)/\partial_{ij} = \nabla^M v_{T_{i,j+1}} \cdot n_{i,j} = \nabla^M v_{T_{i,j}} \cdot n_{i,j}, \quad j = 1, \ldots, N_i,$$

$$\nabla^M v_{T_{i,j}} = \frac{1}{\sin^2 \theta_{i,j}}[(\partial_{i,j}v - \partial_{i,j+1}v \cos\theta_{i,j})n_{i,j} + (\partial_{i,j+1}v - \partial_{i,j}v\cos\theta_{i,j})n_{i,j+1}].$$

Here $i_j \in v_i$ is a vertex of the triangle $T_{i,j}$, $T_{i,0} = T_{i,N_i}$ and $\partial_{i,N_i+1} = \partial_{i,1}$.

Therefore, the first order approximation of the derivative $\nabla^M v_{T_{i,j}}$ ($i \in G_h$, $j = 1, \ldots, N_i$) is defined by a linear combination of the two quantities $\partial_{i,j}v$ and $\partial_{i,j+1}v$ and the numerical Hamiltonian could be written as

$$\widehat{H}(\{\nabla^M v^{n,l}_{T_{i,j}}\}_{j=\overline{1,N_i}}) = \widetilde{H}(\{\partial_{i,j}v^{n,l}\}_{j=\overline{1,N_i}}), \quad i \in G_h.$$

After all, the scheme (2.7) refers to

$$\begin{cases} v_i^{n,1} = v_i^n - \Delta t\widetilde{H}(\{\partial_{i,j}v^n\}_{j=\overline{1,N_i}}), \quad v_i^0 = u_0(x_i), \\ v_i^{n,2} = \dfrac{3}{4}v_i^n + \dfrac{1}{4}v_i^{n,1} - \dfrac{1}{4}\Delta t\widetilde{H}(\{\partial_{ij}v^{n,1}\}_{j=\overline{1,N_i}}), \\ v_i^{n+1} = \dfrac{1}{3}v_i^n + \dfrac{2}{3}v_i^{n,2} - \dfrac{2}{3}\Delta t\widetilde{H}(\{\partial_{ij}v^{n,2}\}_{j=\overline{1,N_i}}). \end{cases} \tag{2.8}$$

In [9], the authors proved the convergence of a generalized monotone scheme in which the high order Runge-Kutta time discretization was applied. Apparently, Assumption 1 on the time discretization in [9] is satisfied by the scheme (2.8). At the same time, from the relation $\Delta t \leqslant ch$ for the time-spacial step (CFL condition), Assumption 2 in [9] is also satisfied with a time step Δt small enough. From Theorem 3.1 of [9], the following result on convergence is true for the scheme (2.8) (and therefore the scheme (2.7)).

Theorem 2.1. *Assume that the assumptions* (A_1) *and* (A_2) *are satisfied for the Hamilton-Jacobi equation* (1.1), (1.2), *and the numerical Hamiltonian* $\widehat{H}(\widetilde{H})$ *is a Lipschitz continuous function satisfying monotonicity and consistency. Then the following estimate holds for the viscosity solution* u *of* (1.1), (1.2) *and the solution* v_h *of the scheme* (2.7):

For $n = 1, \ldots, N_T$, $i \in G_h$,

$$|v_i^n - u(x_{i,n})| \leqslant Ch^{1/2}. \tag{2.9}$$

Here C *is a positive constant depending on* u_0, T *and* u.

R e m a r k 2.1. Notice that all sorts of numerical Hamiltonians that one knows are actually Lipschitz continuous functions.

Theorem 2.2. *Let assumptions of Theorem* 2.1 *be satisfied. We also assume for the solution of the scheme* (2.6) *that the following inequalities hold at every time level* $t = t^n$, $n = 0, 1, \ldots, N-1$:

$$\sum_{j=1}^{N_i} |\nabla u^{n,l}_{T_{i,j}} - \nabla^M u^{n,l}_{T_{i,j}}| \leqslant C_{n,h}, \quad l = 0, 1, 2, \tag{2.10}$$

where $C_{n,h}$ *is independent on the mesh point. Then the following estimate holds for the solution* u_h *of the adaptive scheme* (2.6) *and the solution* v_h *of the scheme* (2.7)*:*

For $n = 1, \ldots, N_T$, $t \in G_h$,

$$|u^n_i - v^n_i| \leqslant \Delta t L \sum_{k=0}^{n-1} C_{k,h}. \tag{2.11}$$

Here L *is a Lipschitz constant of the numerical Hamiltonian* $\widehat{H}$.

P r o o f. We first estimate $|u^1_i - v^1_i|$, $i \in G_h$. From the Lipschitz continuity and monotonicity of the numerical Hamiltonian and the assumption (2.10), we obtain the estimates

$$\begin{aligned} u^{0,1}_i &= u^0_i - \Delta t \widehat{H}(\{\nabla u^0_{T_{i,j}}\}) \\ &= u^0_i - \Delta t \widehat{H}(\{\nabla^M u_{T^0_{i,j}} + (\nabla u^0_{T_{i,j}} - \nabla^M u_{T^0_{i,j}})\}_{j=\overline{1,N_i}}) \\ &\leqslant u^0_i - \Delta t[\widehat{H}(\{\nabla^M u^0_{T_{i,j}}\}_{j=\overline{1,N_i}}) - LC_{0,h}] \\ &= v^0_i - \Delta t \widehat{H}(\{\nabla^M v^0_{T_{i,j}}\}_{j=\overline{1,N_i}}) + \Delta t L C_{0,h} = v^{0,1}_i + \Delta t L C_{0,h} =: w^{0,1}_i, \end{aligned} \tag{2.12}$$

$$\begin{aligned} u^{0,2}_i &= \frac{3}{4} u^0_i + \frac{1}{4} u^{0,1}_i - \frac{1}{4}\Delta t \widehat{H}(\{\nabla u^{0,1}_{T_{i,j}}\}_{j=\overline{1,N_i}}) \\ &\leqslant \frac{3}{4} v^0_i + \frac{1}{4} u^{0,1}_i - \frac{1}{4}\Delta t[\widehat{H}(\{\nabla^M u^{0,1}_{T_{i,j}}\}_{j=\overline{1,N_i}}) - LC_{0,h}] \\ &\leqslant \frac{3}{4} v^0_i + \frac{1}{4}[w^{0,1}_i - \Delta t \widehat{H}(\{\nabla^M w^{,1}_{T_{i,j}}\}_{j=\overline{1,N_i}})] + \frac{1}{4}\Delta t L C_{0,h} \\ &= \frac{3}{4} v^0_i + \frac{1}{4} v^{0,1}_i - \frac{1}{4}\Delta t \widehat{H}(\{\nabla^M u^{0,1}_{T_{i,j}}\}_{j=\overline{1,N_i}}) + \frac{1}{2}\Delta t L C_{0,h} \\ &= v^{0,2}_i + \frac{1}{2}\Delta t L C_{0,h} =: w^{0,2}_i, \end{aligned} \tag{2.13}$$

$$(2.14)\qquad \begin{aligned} u_i^1 &= \frac{1}{3}u_i^0 + \frac{2}{3}u_i^{0,2} - \frac{2}{3}\Delta t\widehat{H}(\{\nabla u_{T_{i,j}}^{0,2}\}_{j=\overline{1,N_i}}) \\ &\leqslant \frac{1}{3}v_i^0 + \frac{2}{3}u_i^{0,2} - \frac{2}{3}\Delta t[\widehat{H}(\{\nabla^M u_{T_{i,j}}^{0,2}\}_{j=\overline{1,N_i}}) - LC_{0,h}] \\ &\leqslant \frac{1}{3}v_i^0 + \frac{2}{3}[w_i^{0,2} - \Delta t\widehat{H}(\{\nabla^M w_{T_{i,j}}^{0,2}\}_{j=\overline{1,N_i}})] + \frac{2}{3}\Delta tLC_{0,h} \\ &= \frac{1}{3}v_i^0 + \frac{2}{3}v_i^{0,2} - \frac{2}{3}\Delta t\widehat{H}(\{\nabla v_{T_{i,j}}^{0,2}\}_{j=\overline{1,N_i}}) + \Delta tLC_{0,h} = v_i^1 + \Delta tLC_{0,h}. \end{aligned}$$

After all, the inequality $u_i^1 \leqslant v_i^1 + \Delta tLC_{0,h}$ has been proved. The inequality $u_i^1 \geqslant v_i^1 - \Delta tLC_{0,h}$ could be verified similarly. Now let $w_i^n = v_i^n + \Delta tL\sum\limits_{k=0}^{n-1} C_{k,h}$ and apply the induction on n. From the induction assumption and the conditions of the theorem, the following inequalities are satisfied:

$$(2.15)\qquad \begin{aligned} u_i^{n,1} &\leqslant u_i^n - \Delta t[\widehat{H}(\{\nabla^M u_{T_{i,j}}^n\}_{j=\overline{1,N_i}}) - LC_{n,h}] \\ &\leqslant w_i^n - \Delta t\widehat{H}(\{\nabla^M w_{T_{i,j}}^n\}_{j=\overline{1,N_i}}) + \Delta tLC_{n,h} \\ &= v_i^n - \Delta t\breve{H}(\{\nabla^M v_{T_{i,j}}^n\}_{j=\overline{1,N_i}}) + \Delta tL\sum_{k=0}^{n} C_{k,h} \\ &= v_i^{n,1} + \Delta tL\sum_{k=0}^{n} C_{k,h} =: w_i^{n,1}, \end{aligned}$$

$$(2.16)\qquad \begin{aligned} u_i^{n,2} &\leqslant \frac{3}{4}u_i^n + \frac{1}{4}u_i^{n,1} - \frac{1}{4}\Delta t[\widehat{H}(\{\nabla^M u_{T_{i,j}}^{n,1}\}_{j=\overline{1,N_i}}) - LC_{n,h}] \\ &\leqslant \frac{3}{4}w_i^n + \frac{1}{4}[w_i^n - \Delta t\widehat{H}(\{\nabla^M w_{T_{i,j}}^{n,1}\}_{j=\overline{1,N_i}}) - LC_{n,h}] \\ &= \frac{3}{4}v_i^n + \frac{1}{4}v_i^{n,1} - \frac{1}{4}\Delta t\widehat{H}(\{\nabla^M v_{T_{i,j}}^n\}_{j=\overline{1,N_i}}) + \Delta tL\sum_{k=0}^{n-1} C_{k,h} + \frac{1}{2}\Delta tLC_{n,h} \\ &= v_i^{n,2} + \Delta tL\sum_{k=0}^{n-1} C_{k,h} + \frac{1}{2}\Delta tLC_{n,h} =: w_i^{n,2}, \end{aligned}$$

$$(2.17)\qquad \begin{aligned} u_i^{n+1} &\leqslant \frac{1}{3}u_i^n + \frac{2}{3}u_i^{n,2} - \frac{2}{3}\Delta t[\widehat{H}(\{\nabla^M u_{T_{i,j}}^{n,2}\}_{j=\overline{1,N_i}}) - LC_{n,h}] \\ &\leqslant \frac{1}{3}w_i^n + \frac{2}{3}[w_i^{n,2} - \Delta t\widehat{H}(\{\nabla^M w_{T_{i,j}}^{n,2}\}_{j=\overline{1,N_i}})] + \frac{2}{3}\Delta tLC_{n,h} \\ &= \frac{1}{3}v_i^n + \frac{2}{3}v_i^{n,2} - \frac{2}{3}\Delta t\widehat{H}(\{\nabla^M v_{T_{i,j}}^{n,2}\}_{j=\overline{1,N_i}}) + \Delta tL\sum_{k=0}^{n} C_{k,h} \\ &= v_i^{n+1} + \Delta tL\sum_{k=0}^{n} C_{k,h}. \end{aligned}$$

Therefore, the inequality $u_i^{n+1} \leqslant v_i^{n+1} + \Delta t L \sum\limits_{k=0}^{n} C_{k,h}$, $i \in G_h$, was proved. The inequality $u_i^{n+1} \geqslant v_i^{n+1} - \Delta t L \sum\limits_{k=0}^{n} C_{k,h}$ is proved similarly. □

The solution v_h of the scheme (2.7) converges to the solution and, therefore, the solution u_h of the adaptive scheme converges to the viscosity solution of the equation (1.1), (1.2) under the condition that the right-hand side of (2.11) converges to zero as h tends to zero, which depends on the selection of the combining coefficient.

Theorem 2.3. *Assume that the conditions of Theorem* 2.2 *are satisfied. If the first order approximation of derivative is applied to singular parts of the solution of the HJ equation (blending coefficient $\lambda_i = 0$), then the adaptive scheme* (2.6) *converges.*

P r o o f. From the definition of the approximation of derivative, the following estimate for the solution of the scheme (2.6) holds in smooth regions of the solution:

$$\sum_{j=1}^{N_i} |\nabla u_{T_{i,j}}^{n,l} - \nabla^M u_{T_{i,j}}^{n,l}| \leqslant O(h). \tag{2.18}$$

On the other hand, in case that first order approximations are applied to singular parts of the solution, the equality

$$\sum_{j=1}^{N_i} |\nabla u_{T_{i,j}}^{n,l} - \nabla^M u_{T_{i,j}}^{n,l}| = 0 \tag{2.19}$$

is satisfied. Therefore, we obtain the following estimate from the inequality (2.11):

For $n = 1, \ldots, N_T$, $i \in G_h$,

$$|u_i^n - v_i^n| \leqslant \Delta t L \sum_{j=1}^{N_T - 1} C_{k,h} \leqslant \Delta t L N_T C_1 h = C_2 h. \tag{2.20}$$

Applying the above inequality and the estimate (2.9), we obtain the inequality

$$|u_i^n - u(x_i, t_n)| \leqslant |u_i^n - v_i^n| + |v_i^n - u(x_i, t_n)| \leqslant C h^{1/2}. \tag{2.21}$$

After all, in case that the first order approximations are applied to singular parts of the solution of the HJ equation, the adaptive scheme (2.6) converges. □

3. Adaptive WENO schemes on triangular meshes

We construct adaptive schemes of WENO type on triangular meshes in which first order approximations are partly applied near singular points instead of WENO approximations.

3.1. Singularity indicator of the solution. The way of combining WENO and first order approximations at a mesh point depends highly on the smoothness of the solution near the point. Ahead of composing adaptive algorithms, we introduce the concept of singularity indicator which characterizes the singularity of the solution near a given point.

3.1.1. One-dimensional case. We denote the partition of $\mathbb{R}$ by $G_h = \{x_i\,;\ i = 0, \pm 1, \ldots\}$, $h = \sup_i (x_i - x_{i-1})$, and identify every node with its index in below.

For the mesh function u_h defined on G_h, we define the singularity indicator S_i at the point i as

$$S_i = \frac{\alpha_i}{\alpha_i + \beta_i}, \quad i = 0,\ \pm 1, \ldots \tag{3.1}$$

Here

$$\alpha_i = \max\{\gamma_i/\gamma_{i-1}, \gamma_i/\gamma_{i+1}\},\ \beta_i = (u'_{\max} - u'_{\min})^2/\gamma_i,\ u^{\pm}_{i,\mathrm{mono}} = \frac{u_{i\pm 1} - u_i}{x_{i\pm 1} - x_i},$$
$$\gamma_i = (u^{+}_{i,\mathrm{mono}} - u^{-}_{i,\mathrm{mono}})^2 + \varepsilon,\ u'_{\max} = \sup_{i=0,\pm 1,\ldots} u^{\pm}_{i,\mathrm{mono}},\ u'_{\min} = \inf_{i=0,\pm 1,\ldots} u^{\pm}_{i,\mathrm{mono}}$$

and ε is a sufficiently small positive constant taken as $\varepsilon \approx 10^{-6}$ in practice.

In general, the viscosity solution of the Hamilton-Jacobi equation is Lipschitz continuous and therefore the set of singular points of the solution consists of isolated points. Accordingly, the singularity indicator S_i has the following properties:

▷ $0 \leqslant S_i \leqslant 1$,
▷ $S_i \sim O(h^2)$ in smooth regions of the solution,
▷ $S_i \approx 1$ near a singularity.

The singularity indicator is estimated by $(u''_M/u'_M)^2 h^2$ in smooth regions, where $u'_M = u'_{\max} - u'_{\min}$ and u''_M is the upper bound of the second order derivative of the solution.

3.1.2. Singularity indicator on triangular mesh. Let us define the singularity indicator for a mesh function $\{u_p, p \in G_h\}$. We first enumerate the neighboring nodes of the point $p \in G_h$ and denote them by p_i, $i = 1, \ldots, n_p$. The first order approximation of the directional derivative from the point p towards p_i is denoted by $u'_{pp_i} = (u_{p_i} - u_p)/|pp_i|$.

(i) Setting up angular sectors. We first find a neighboring point of the point $p \in G_h$, denoted by p'_1, where $|u'_{pp'_1}|$, $i = 1, \dots, n_p$. If the number of neighboring points n_p is an even one, then setting the half line pp'_1 as a criterion, we divide the angle (2π) around the point p equally into n_p sectors. If n_p is an odd number, the angle around the point p is divided into $n_p + 1$ sectors and hereafter, all discussions will be the same as in the case that n_p is an even number with the exception of using $n_p + 1$ in place of n_p. Now let n_p be an even number. We select a point on every angle-dividing half line within triangles with the vertex p and denote these points by p'_i, $i = 2, \dots, n_p$, which are in turn enumerated in the counterclockwise direction with the starting point p'_1.

(ii) Approximation of pp'_i-directional derivative $u'_{pp'_i}$ $(i = 1, \dots, n_p)$. If there exists any neighboring point p_j of the node p on the half line pp'_i, we define the approximation of the pp'_i-directional derivative as $u'_{pp'_i} = u'_{pp'_j}$. Now assume that there does not exist any neighboring point of the node p on the half the line pp'_i. If the triangle which the half line pp'_i intersects has three vertices p, p_j, p_k, then using these three interpolation points, we make a linear interpolation function with the interpolation function values u_p, u_{p_j}, u_{p_k}. Then we define the approximation of the pp'_i-directional derivative $u'_{pp'_i}$ as the pp'_i-directional derivative of this interpolation function, which is equal to the inner product between the gradient of the interpolation function and pp'_i-directional unit vector.

(iii) Definition of the singularity indicator. We define the singularity indicator S_p of a mesh function u_p, $p \in G_h$, at the point $p \in G_h$ as

$$S_p = \frac{\alpha_p}{\alpha_p + \beta_p}, \quad p \in G_h. \tag{3.2}$$

Here $\alpha_p = \max_{i=1,\dots,n_p} \{\gamma_p/\gamma_{p_i}\}$, $\quad \beta_p = u'^2_{\max}/\gamma_p$,

$$\gamma_p = \max_{i=1,\dots,n_p/2} (u'_{pp'_i} + u'_{pp'_{i+n_p/2}})^2 + \varepsilon, \quad u'^2_{\max} = \sup_{p \in G_h} \gamma_p.$$

Considering the property of the viscosity solution of the Hamilton-Jacobi equation, we find out that the singularity indicator S_p has the same properties as in the one-dimensional case.

First of all, the singularity indicator S_p is $O(h^2)$ in smooth regions of the solution. This fact is directly derived from the definition of the singularity indicator under the relationship which holds in smooth regions of the solution:

$$\gamma_p = O(h^2). \tag{3.3}$$

The above relation (3.3) can be obtained from the estimate on the approximation of the directional derivative $u'_{pp'_i}(u'_{pp'_{i+n_p/2}})$. For this, assume that $\gamma_p = (u'_{pp'_i} + u'_{pp'_{i+n_p/2}})^2$ (ε is neglected during discussion) for some i ($1 \leqslant i \leqslant n_p/2$) and the three vertices of the triangle where the half line pp'_i intersects are p, p_j and p_k. Now for $h'_i = |x_p - x_{p'_i}|$, there exist $\lambda_1, \lambda_2 \geqslant 0$, $\lambda_1 + \lambda_2 = 1$ such that $x_{p'_i} = \lambda_1 x_{p_j} + \lambda_2 x_{p_k}$,

$$u'_{pp'_i} = \frac{(\lambda_1 u_{p_j} + \lambda_2 u_{p_k}) - u_p}{h'_i} = \frac{(\lambda_1 u_{p_j} + \lambda_2 u_{p_k}) - u(x_{p'_i})}{h'_i} + \frac{u(x_{p'_i}) - u_p}{h'_i}. \tag{3.4}$$

The second term of the right hand side in (3.4) is estimated as $\nabla_{pp'_i} u(x_p) + O(h'_i)$. On the other hand, considering the equalities

$$\begin{aligned} u_{p_j} &= u(x_{p'_i}) + \lambda_2 \nabla u(x_{p'_i}) \cdot (x_{p_j} - x_{p_k}) + O((x_{p_j} - x_{p_k})^2), \\ u_{p_k} &= u(x_{p'_i}) + \lambda_1 \nabla u(x_{p'_i}) \cdot (x_{p_k} - x_{p_j}) + O((x_{p_k} - x_{p_j})^2), \end{aligned}$$

and the assumption that the triangulation is regular, the first term of the righthand side in (3.4) is estimated as $O(x_{p_j} - x_{p_k})$. For $u'_{pp'_{i+n_p/2}}$, the approximation of the $pp'_{i+n_p/2}$-directional derivative opposite to the pp'_i-direction, we perform similar discussions. Considering the equality $\nabla_{pp'_i} u(x_p) + \nabla_{pp'_{i+n_p/2}} u(x_p) = 0$, we finally conclude that the relationship (3.3) holds in smooth regions of the solution.

The singularity indicator S_p is also close to 1 in singular parts of the solution. In fact, if a singular point of the Lipschitz continuous viscosity solution falls in the neighborhood of the point p which is a union of all triangles with the vertex p, we notice from the definition that $\gamma_p \approx O(1)$, $\alpha_p \approx O(h^{-2})$ and $\beta_p \approx O(1)$, and therefore, $\alpha_p \gg \beta_p$ and $S_p \approx 1$.

3.2. Adaptive scheme of WENO type. Using the singularity indicator, we first define a scheme of WENO + first order monotone type.

Algorithm 3.1: WENO+First Order Monotone.

(i) Approximation of derivative. The approximations of left and right derivatives at the point $i \in G_h$ are as follows:

$$u^-_{x,i} = (1 - S_i) u^-_{i,\mathrm{WENO}} + S_i u^-_{i,\mathrm{mono}}, \quad u^+_{x,i} = (1 - S_i) u^+_{i,\mathrm{WENO}} + S_i u^+_{i,\mathrm{mono}}. \tag{3.5}$$

Here S_i, $u^{\pm}_{i,\mathrm{WENO}}$ and $u^{\pm}_{i,\mathrm{mono}}$ refer to the singularity indicator, high order WENO and first order approximations on the left and right-biased stencils at the node i, respectively.

(ii) The semi-discrete form of the scheme is

$$\frac{\mathrm{d}u_i(t)}{\mathrm{d}t} + \widehat{H}(u_{x,i}^-, u_{x,i}^+) = 0, \quad i = 0, \pm 1, \dots \tag{3.6}$$

Here $\widehat{H}$ is a numerical Hamiltonian satisfying consistency and monotonicity.

Using the SSP third order Runge-Kutta method, we complete the full-discrete scheme. The approximation of derivative introduced in (3.5) takes the high order WENO type in smooth regions of the solution and the first order one in singular parts of the solution. After all, the convergence of the scheme constructed above is derived from Theorem 2.3. Such a conclusion will be demonstrated through numerical experiments. We can construct similar schemes on triangular meshes for two-dimensional problems.

On the other hand, the high order scheme gives more accurate approximation results than the first order monotone one by its high order accuracy. Using only the first order approximation in singular parts of the solution as in (3.5) may cause rather poor numerical approximation results. In order to assure not only convergence but also more accurate numerical results, it is desirable to use as high order approximation as possible. Therefore, the blending manner of WENO and first order approximations as in (3.5) is apparently not optimal. After all, a more careful consideration for approximations of the derivative is needed in singular parts of the solution.

Using the fact that the first order monotone scheme always converges, we may ascribe the problem of constructing the scheme at singular point $x_i \in R$ to the analysis of a local Riemann problem with left and right derivatives $u_{i,\text{mono}}^-$ and $u_{i,\text{mono}}^+$. Then the local solution of the Riemann problem near the point $x_i \in R$ heavily depends on convexity/concavity of the Hamiltonian H in the interval $[u_{i,\text{mono}}^-, u_{i,\text{mono}}^+](u_{i,\text{mono}}^-, u_{i,\text{mono}}^+)$. If the Hamiltonian H is strictly convex, concave or linear in this interval, then the initial state is still preserved as the isolated singularity (kink) or is rather smoothen as the time evolves. In this case, we ought to use the high order WENO approximation at the point $x_i \in R$. If the Hamiltonian H is nonconvex in the interval $[u_{i,\text{mono}}^-, u_{i,\text{mono}}^+](u_{i,\text{mono}}^-, u_{i,\text{mono}}^+)$, a new singularity corresponding to the rarefaction wave in the conservation law is developed in the viscosity solution as the time evolves and the high order scheme occasionally fails to capture such a singularity. Thus, this leads to the result that the approximate solution fails to converge. In this case, we must apply the first order approximation for the convergent scheme. Based on the above discussion, we propose adaptive WENO schemes in which first order approximations are partly applied.

Algorithm 3.2: Adaptive WENO scheme (1-dimensional).

(i) Approximation of derivative. For the upper bound δ of the singularity indicator in the smooth region of the solution, we define approximations of derivative $u_{x,i}^{\pm}$ as follows:

– If $S_i \leqslant \delta$, then $u_{x,i}^{\pm} = u_{i,\mathrm{WENO}}^{\pm}$.

– In case of $S_i > \delta$, we first divide $\mathbb{R}$ into intervals in which the Hamiltonian H is strictly convex, concave or linear.

  ▷ If both the first order approximations $u_{i,\mathrm{Mono}}^{-}$ and $u_{i,\mathrm{Mono}}^{+}$ fall into the same divided interval, we take $u_{x,i}^{\pm} = u_{i,\mathrm{WENO}}^{\pm}$.

  ▷ Otherwise: If both $u_{i,\mathrm{mono}}^{-}$ ($u_{i,\mathrm{mono}}^{+}$) and $u_{i,\mathrm{WENO}}^{-}$ ($u_{i,\mathrm{WENO}}^{+}$) fall into the same divided interval, $u_{x,i}^{-} = u_{i,\mathrm{WENO}}^{-}$ ($u_{x,i}^{+} = u_{i,\mathrm{WENO}}^{+}$). Otherwise, $u_{x,i}^{-} = u_{i,\mathrm{mono}}^{-}$ ($u_{x,i}^{+} = u_{i,\mathrm{mono}}^{+}$).

(ii) Use the SSP third order Runge-Kutta method for the time discretization.

Remark 3.1. The above adaptive approximation of the derivative was derived from the idea in Section 2. Especially in the case that the singularity indicator is less than the threshold δ, the high order WENO approximation was applied, considering that the solution is smooth near the point $i \in G_h$. On the other hand, our numerical experiments show that numerical solutions depend relatively stably on the selection of the threshold δ.

Now we construct the adaptive scheme of WENO type on triangular meshes.

Algorithm 3.3: Adaptive WENO scheme on triangular meshes.

(i) Perform WENO approximations of derivative on triangular meshes. The WENO and first order approximations of derivative in the triangle $p_i p p_{i+1}$are denoted by $\nabla^W u_{p,i}$ and $\nabla^M u_{p,i}$ ($i = 1, \ldots, n_p$), respectively.

(ii) Approximation of derivative. For the upper bound δ of the singularity indicator in the smooth region of the solution, we define the approximation of the derivative $\nabla u_{p,i}$ ($p \in G_h$, $i = 1, \ldots, n_p$) as follows:

– If $S_p \leqslant \delta$, then $\nabla u_{p,i} = \nabla^M u_{p,i}$ ($i = 1, \ldots, n_p$).

– In case that $S_p > \delta$, we first divide $\mathbb{R}^2$ into subregions in which Hamiltonian H is strictly convex, concave or linear.

  ▷ If all the first order approximations $\nabla^M u_{p,i}$, $i = 1, \ldots, n_p$, fall into the same subregion, we take $\nabla u_{p,i} = \nabla^W u_{p,i}$, $i = 1, \ldots, n_p$.

  ▷ Otherwise: If both $\nabla^M u_{p,i}$ and $\nabla^W u_{p,i}$ ($i = 1, \ldots, n_p$) fall into the same subregion, $\nabla u_{p,i} = \nabla^W u_{p,i}$. Otherwise, $\nabla u_{p,i} = \nabla^M u_{p,i}$.

(iii) The semi-discrete form of the adaptive WENO scheme is

$$\frac{\mathrm{d}u_p(t)}{\mathrm{d}t} + \widehat{H}(\nabla u_{p,1}, \ldots, \nabla u_{p,n_p}) = 0. \tag{3.7}$$

The numerical Hamiltonian $\widehat{H}(\cdot)$ is, see [1],

$$\begin{aligned}
&\widehat{H}(\nabla u_{p,i}, \ldots, \nabla u_{p,n_p}) \\
&\qquad = H\Big(\frac{\sum_{i=1}^{n_p} \theta_i \nabla u_{p,i}}{2\pi}\Big) - \frac{\widehat{L}_H}{\pi} \sum_{i=1}^{n_p} \varphi_{i+1/2} \Big(\frac{\nabla u_{p,i} + \nabla u_{p,i+1}}{2}\Big) \cdot \vec{n}_{i+1}, \\
&\varphi_{i+1/2} = \tan(\theta_i/2) + \tan(\theta_{i+1}/2), \quad \theta_i = \angle p_i p p_{i+1}, \\
&\quad \widehat{L}_H = \max\Big\{\max_{i=1,\ldots,n_p} |H_1'(\nabla u_{p,i})|, \max_{i=1,\ldots,n_p} |H_2'(\nabla u_{p,i})|\Big\}.
\end{aligned}$$

Here $\vec{n}_i$ is the pp_i-directional unit vector and H_1' (H_2') is the partial derivative (or Lipschitz constant) with respect to the first (second) variable of the Hamiltonian H. Using the SSP third order Runge-Kutta time discretization, we complete the full scheme.

4. Numerical examples

In this section, we show the convergence and effectiveness of adaptive schemes of WENO type through numerical examples.

Example 4.1. Consider the linear problem

$$\begin{cases} u_t + u_x = 0, \\ u(x,0) = u_0(x - 0.5), \end{cases} \tag{4.1}$$

where u_0 is a periodic function (of period 2) defined in Example 5.1 of [9].

As we know from the characteristic method, the solution of the equation (4.1) is $u(x,t) = u_0(x - t - 0.5)$. The results by Algorithm 3.1 combining the fifth order WENO approximation with the first order monotone one at $t = 2$ (left) and 8 (right) are displayed in Fig. 1. In this figure, solid lines denote the solution of the equation (4.1). As we can see, the numerical solutions by Algorithm 3.2 achieve much more accurate approximations in singular parts of the solution than the first order monotone one.

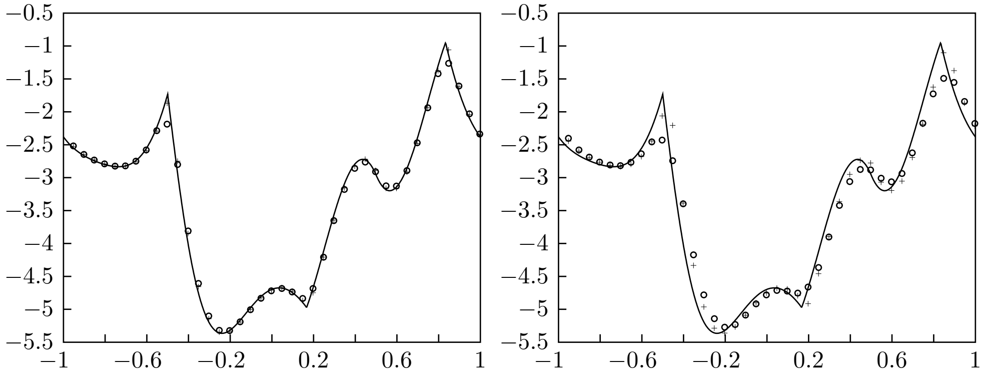

Figure 1. "+": Algorithm 3.1, "∘": the first order monotone approximation.

E x a m p l e 4.2. Consider the problem with nonconvex Hamiltonian

$$\begin{cases} u_t + u_x^3/3 = 0, \\ u(x,0) = -\cos(\pi x)/\pi, \quad -1 \leqslant x \leqslant 1. \end{cases} \tag{4.2}$$

Table 1 shows numerical results by the fifth order WENO schemes and adaptive WENO schemes ($t = 0.2$).

	WENO scheme				Adaptive scheme				
N	L^1-error	order	L^∞-error	order	L^1-error	order	L^∞-error	order	δ
40	2.839e − 05		1.106e − 04		2.838e − 05		1.104e − 04		0.1
					3.004e − 05		1.102e − 04		0.01
					3.004e − 05		1.101e − 04		0.001
80	1.787e − 06	3.99	1.106e − 04	3.51	1.787e − 06	3.99	9.688e − 06	3.51	0.1
					1.787e − 06	4.07	9.688e − 06	3.51	0.01
					1.881e − 06	3.99	9.688e − 06	3.51	0.001
160	9.679e − 08	4.20	8.019e − 07	3.59	9.683e − 08	4.20	8.019e − 07	3.59	0.1
					9.683e − 08	4.20	8.019e − 07	3.59	0.01
					9.683e − 08	4.20	8.019e − 07	3.59	0.001
320	3.717e − 09	4.70	3.474e − 08	4.53	3.717e − 09	4.70	9.688e − 06	4.53	0.1
					3.717e − 09	4.70	3.474e − 08	4.53	0.01
					3.717e − 09	4.70	3.474e − 08	4.53	0.001

Table 1. L^1 and L^∞-errors for fifth order WENO and adaptive schemes.

As the table shows, L^1 and L^∞-errors of both the schemes are comparable. Furthermore, numerical solutions by the adaptive scheme are very stable with respect to the selection of a threshold δ which is the upper bound of the singularity indicator.

E x a m p l e 4.3. Consider the problem with the Hamiltonian and initial function

$$
(4.3) \qquad H(v) = \begin{cases} 0, |v| > \dfrac{1}{2}, \\[2ex] -\cos(\pi v), |v| \leqslant \dfrac{1}{2}, \end{cases} \qquad u_0(x) = \begin{cases} -x, x \leqslant 0, \\ x, x > 0, \end{cases}
$$

$$
(4.4) \qquad H(v) = \begin{cases} 0, |v| > 0.2, \\ -\cos(2.5\pi v), |v| < 0.2, \end{cases} \qquad u_0(x) = \begin{cases} -x, x \leqslant 0, \\ x, x > 0. \end{cases}
$$

The pure high order WENO schemes fail to converge for both the problems. Fig. 2 shows the numerical results by Algorithm 3.2. As we can see, the numerical solution by the adaptive WENO scheme converges to the viscosity solution of the Hamilton-Jacobi equation.

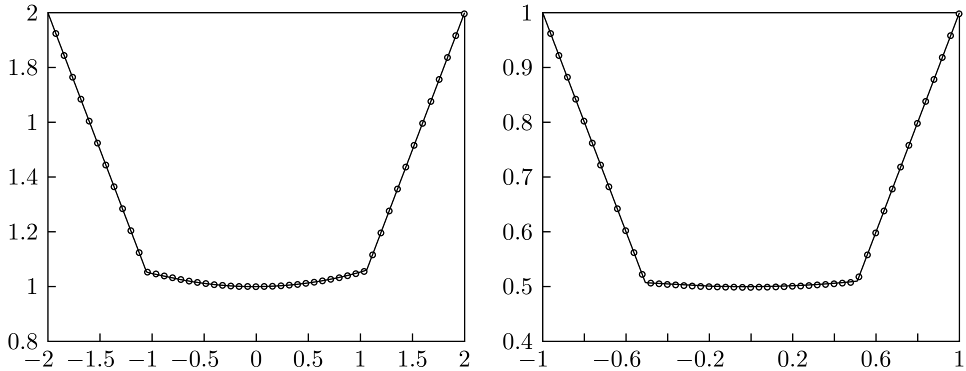

Figure 2. The numerical results for the problems (4.3) (left) and (4.4) (right), the solid line-viscosity solution, "○"-Algorithm 3.2.

E x a m p l e 4.4. Now we consider the 2D HJ equation

$$
(4.5) \qquad \begin{cases} u_t - \cos(u_x + u_y + 1) = 0, \quad (x, y) \in [-2, 2] \times [-2, 2], \\ u(x, y, 0) = -\cos \dfrac{\pi(x + y)}{2}. \end{cases}
$$

We computed the viscosity solution of the 2-dimensional Hamilton-Jacobi equation (4.5) with nonconvex Hamiltonian using the Adaptive WENO scheme by Algorithm 3.3.

Table 2 shows L^1 and L^∞-errors of the third order WENO and adaptive schemes for the equation (4.5) at time $t = 0.5/\pi^2$. L^1 and L^∞-errors of the adaptive WENO scheme with a reasonably selected threshold δ almost agree with errors of the WENO scheme. The numerical solutions by the adaptive scheme are stable with respect to the selection of threshold δ as in Example 4.2.

N	WENO scheme L^1-error order	L^∞-error order	Adaptive scheme L^1-error	L^∞-error	δ
2×10^2	0.0167	2.935e − 03	0.0167	2.935e − 03	1
			0.0887	0.0418	0.1
			0.1226	0.0418	0.01
2×20^2	3.613e − 03 2.21	6.871e − 04 2.09	3.613e − 03	6.871e − 04	0.5
			4.211e − 03	3.986e − 03	0.1
			0.0186	0.0163	0.01
2×40^2	4.875e − 04 2.89	1.314e − 04 2.38	4.872e − 04	1.314e − 04	0.05
			4.872e − 04	1.314e − 04	0.1
			5.643e − 03	3.845e − 03	0.01
2×80^2	6.372e − 05 2.93	1.936e − 05 2.76	6.372e − 05	1.936e − 05	$0.01\sim 0.1$

Table 2. L^1 and L^∞-errors of the third order WENO and adaptive schemes.

Example 4.5. Consider the 2D HJ equation

$$u_t+\sin(u_x)+\cos(u_y)=0,\quad (x,y)\in(-2,2)\times(-2,2),\quad t>0, \tag{4.6}$$

with the initial condition

$$u(x,y,0)=\begin{cases}\dfrac{\pi(14r-13)}{4}, & r\leqslant\dfrac12,\\[2mm] \dfrac{\pi(14r-13)}{4}+2\sin(10\pi r), & \dfrac12\leqslant r<1,\ r=\sqrt{x^2+y^2},\\[2mm] \dfrac{\pi r}{4}, & r>1,\end{cases} \tag{4.7}$$

and the homogeneous Neumann boundary conditions for u_x and u_y

$$\begin{cases}u_{xx}(-2,y,t)=u_{xx}(2,y,t)=0 & \forall\, t,\ \forall\, y\in[-2,2],\\ u_{yy}(x,-2,t)=u_{yy}(x,2,t)=0 & \forall\, t,\ \forall\, y\in[-2,2],\end{cases} \tag{4.8}$$

Fig. 3 shows the contour lines of numerical solutions computed by the third order WENO scheme and the adaptive scheme of the third order WENO type by Algorithm 3.3 on the triangular mesh with 2×201^2 elements at time $t=2$. For this problem, we divided the 2-dimensional domain $\mathbb{R}^2$ into the subregions $(m\pi,(m+1)\pi)\times(n\pi/2,(n+1)\pi/2)$, $m,n\in\mathbb{Z}$, across each of which $H(v)$ is strictly convex or concave. As we can see in Fig. 3, the approximate solution by the WENO scheme fails to converge to the solution of the problem (4.6)–(4.8). On the other hand, as the contour lines show, the approximate solution by the adaptive scheme converges to the viscosity solution of the Hamilton-Jacobi equation (4.6)–(4.8).

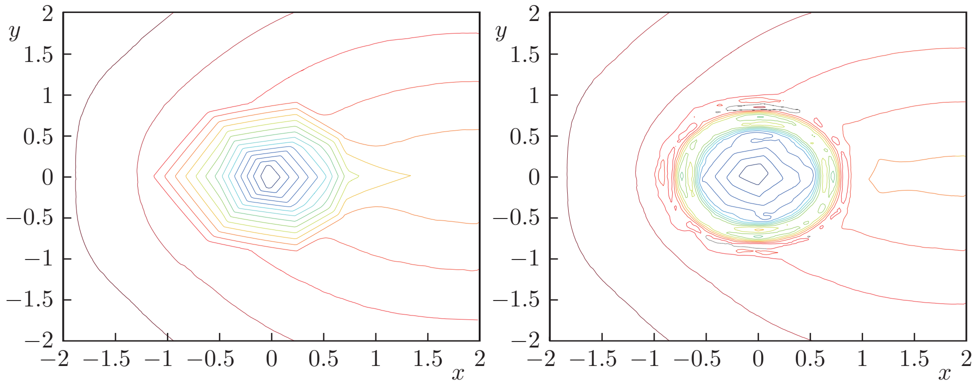

Figure 3. Contour lines ($t = 2$) of approximate solutions by the adaptive (left) and third order WENO (right) schemes.

5. Conclusion

We have developed the method of constructing convergent schemes of high order type for the time-dependent Hamilton-Jacobi equation on triangular meshes and proposed a sort of adaptive algorithms for reasonable combining high WENO and first order monotone schemes.

References

[1] *R. Abgrall*: Numerical discretization of the first-order Hamilton-Jacobi equation on triangular meshes. Commun. Pure Appl. Math. *49* (1996), 1339–1373. zbl MR doi

[2] *O. Bokanowski, M. Falcone, S. Sahu*: An efficient filtered scheme for some first order time-dependent Hamilton-Jacobi equations. SIAM J. Sci. Comput. *38* (2016), A171–A195. zbl MR doi

[3] *X. Cai, J. Qiu, J. Qiu*: Finite volume HWENO schemes for nonconvex conservation laws. J. Sci. Comput. *75* (2018), 65–82. zbl MR doi

[4] *M. G. Crandall, P.-L. Lions*: Two approximations of solutions of Hamilton-Jacobi equations. Math. Comput. *43* (1984), 1–19. zbl MR doi

[5] *H. Feng, C. Huang, R. Wang*: An improved mapped weighted essentially non-oscillatory scheme. Appl. Math. Comput. *232* (2014), 453–468. zbl MR doi

[6] *S. Gottlieb, C.-W. Shu, E. Tadmor*: Strong stability-preserving high-order time discretization methods. SIAM Rev. *43* (2001), 89–112. zbl MR doi

[7] *C. Huang*: WENO scheme with new smoothness indicator for Hamilton-Jacobi equation. Appl. Math. Comput. *290* (2016), 21–32. zbl MR doi

[8] *G.-S. Jiang, D. Peng*: Weighted ENO schemes for Hamilton-Jacobi equations. SIAM J. Sci. Comput. *21* (2000), 2126–2143. zbl MR doi

[9] *K. Kim, Y. Li*: Construction of convergent high order schemes for time dependent Hamilton-Jacobi equations. J. Sci. Comput. *65* (2015), 110–137. zbl MR doi

[10] *D. Levy, S. Nayak, C.-W. Shu, Y.-T. Zhang*: Central WENO schemes for Hamilton-Jacobi equations on triangular meshes. SIAM J. Sci. Comput. *28* (2006), 2229–2247. zbl MR doi

[11] *A. M. Oberman, T. Salvador*: Filtered schemes for Hamilton-Jacobi equations: A simple construction of convergent accurate difference schemes. J. Comput. Phys. *284* (2015), 367–388. zbl MR doi
[12] *S. Osher, C.-W. Shu*: High-order essentially nonoscillatory schemes for Hamilton-Jacobi equations. SIAM J. Numer. Anal. *28* (1991), 907–922. zbl MR doi
[13] *J. Qiu, C.-W. Shu*: Hermite WENO schemes for Hamilton-Jacobi equations. J. Comput. Phys. *204* (2005), 82–99. zbl MR doi
[14] *J.-M. Qiu, C.-W. Shu*: Convergence of high order finite volume weighted essentially nonoscillatory scheme and discontinuous Galerkin method for nonconvex conservation laws. SIAM J. Sci. Comput. *31* (2008), 584–607. zbl MR doi
[15] *C.-W. Shu*: High order weighted essentially nonoscillatory schemes for convection dominated problems. SIAM Rev. *51* (2009), 82–126. zbl MR doi
[16] *Y.-T. Zhang, C.-W. Shu*: High-order WENO schemes for Hamilton-Jacobi equations on triangular meshes. SIAM J. Sci. Comput. *24* (2003), 1005–1030. zbl MR doi
[17] *J. Zhu, J. Qiu*: Hermite WENO schemes for Hamilton-Jacobi equations on unstructured meshes. J. Comput. Phys. *254* (2013), 76–92. zbl MR doi
[18] *J. Zhu, J. Qiu*: A new fifth order finite difference WENO scheme for Hamilton-Jacobi equations. Numer. Method Partial Differ. Equations *33* (2017), 1095–1113. zbl MR doi

Authors' addresses: *Kwangil Kim*, Department of Mathematics, University of Sciences, Wisong Street, Pyongyang 950003, DPR Korea, e-mail: `kwangil@163.com`; *Unhyok Hong*, Institute of Mathematics, State Academy of Sciences, Wisong Street, Pyongyang 950003, DPR Korea, e-mail: `unhyok@163.com`; *Kwanhung Ri*, Department of Mathematics, University of Sciences, Wisong Street, Pyongyang 950003, DPR Korea, e-mail: `kwanhung@163.com`; *Juhyon Yu* (corresponding author), Department of Chemistry, University of Sciences, Wisong Street, Pyongyang 950003, DPR Korea, e-mail: `yujuhy@163.com`.